Paper 152

©Civil-Comp Press, 2012
Proceedings of the Eleventh International Conference
on Computational Structures Technology,
B.H.V. Topping, (Editor),
Civil-Comp Press, Stirlingshire, Scotland

Nonlinear Finite-Element Analysis of the Shear Behaviour of Stud Connectors

Q. Wang[1,2], Y.Q. Liu[1] and J.P. Lebet[2]
[1] Bridge Department, Tongji University, Shanghai, China
[2] Steel Structures Laboratory (ICOM)
École Polytechnique Fédérale de Lausanne (EPFL), Switzerland

Abstract

This paper presents a nonlinear finite element model for a push-out specimen to study on the shear mechanical behaviour of stud connectors. ABAQUS was used to build the numerical models of push-out specimens, in which material nonlinearity of concrete and stud was considered. The calculated results for the push-out specimens were compared with the experimental results for verification. The nonlinear finite-element models after verification can provide a good estimate of the mechanical behaviour of the stud connectors in the push-out tests. An extensive parametric study was conducted to analyse the effects of different concrete strengths, stud diameters and applied tensile forces to the shear behaviour of the stud connectors. The shear resistance of the stud connector increases as the stud diameter and concrete strength increases, and the stud diameter has a greater effect than concrete strength; the shear resistance of stud connector under combined forces decreases as the applied tensile force increases.

Keywords: stud connector, finite element method, push-out tests, combined forces, shear behaviour.

1 Introduction

Composite structures have obvious economic and structural advantages compared with steel structures and concrete structures, respectively. Stud connector is the main connector used in composite structures till now to resist the slip and separation between concrete and steel. Stud connectors normally work under both tensile force and shear force in many practical structures. The tensile force has to be considered when $F_{ten}>0.1P_{Rd}$ [1] and it will influence the shear resistance of stud connectors in a certain range.

Push-out experiment and beam experiment are normally used to measure the mechanical behaviour of stud connectors. Driscoll and Slutter [2,3] gave the conclusion that the results of push-out tests are the lower limit to estimate the shear resistance of stud connectors through analyzing both kinds of experiments. All equations in current design codes [1,4,5] to calculate the shear resistance of stud connectors are empirical formula based on the statistical analysis of push-out tests results.

Push-out experiment provides a convenient way to study the behaviour of shear connector than beam tests, but still costly and time consuming. Many researchers began to investigate the behaviour of stud connectors by using finite element model simulation method, which also can predict the non-linear response and the ultimate load capacity of the push-out test after the comparison with selective experimental results and the verification of simulation method. Ellobody et al [6,7,8] developed an accurate nonlinear finite element model to investigate the mechanical behaviour of stud connectors in solid slabs and precast hollow core slab, the results obtained from FE models were compared with experimental results and design strengths calculated using several design codes. 2009, Nguyen and Kim [9] analyzed large stud connectors of 22mm, 25mm, 27mm and 30mm using nonlinear finite element models and observed that AASHTO LRFD specifications overestimated the capacity of large stud connectors whereas the design rules specified in EC4 were generally conservative for stud diameters of 22, 25 and 27 mm, and unconservative for diameter of 30mm.

The main objective of the paper is to build a nonlinear finite-element model for push-out specimens of stud connectors. Material nonlinear was taken into account and different stud diameters, concrete strengths and tensile forces were calculated. Parametric study on the mechanical behaviour of stud connector was investigated in the nonlinear finite element models.

1 Push-out specimens

Push-out specimens were fabricated according to the standard push-out test specimen in Eurocode 4 [1]. Stud diameter was considered as 22mm, 25mm, stud length was 200mm, concrete strength was and stud of 22mm diameter was applied tensile force at two sides of the specimen as shown in Figure 1 (a).

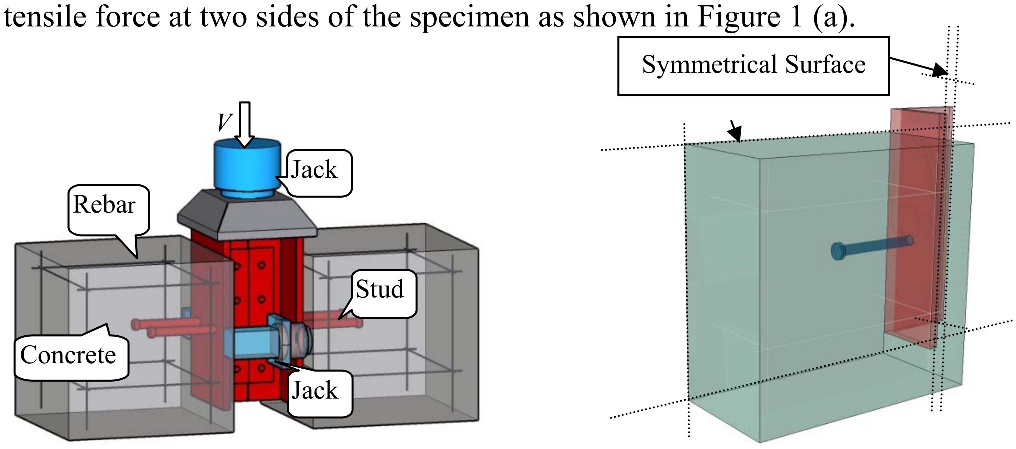

(a) Push-out Specimen (b) 1/4 FE model with ABAQUS

Figure 1. Design of push-out specimen

Specimen			d_s (mm)	h_s (mm)	f_{su} (MPa)	f_{cu} (MPa)	N_s (kN)	V_{su} (kN) Value	Mean Value
Pure Shear	SS-1	1	22	200	465	70.3	0	152.5	208.5
		2						233.9	
		3*						239.0	
	SS-2	1	25				0	266.2	272.7
		2						265.6	
		3*						286.3	
Combined Forces	SS-3	1	22	200	519	62.6	33.2	159.7	176.1
		2						192.4	
	SS-4	1	22				66.3	145.8	154.6
		2						163.3	
The ones with * were tested under cyclic loading									

Table 1. Push-out specimens

In the above table:
d_s: Shank Diameter (mm);
h_s: Stud Height (mm);
f_{su}: Tensile Strength of Studs (MPa);
f_{cu}: Cubic Compressive Strength of Concrete (MPa);
N_s:Tensile force (kN);
V_{su}: Shear Resistance (kN).

3 Analytical Model

3.1 General

The finite element program ABAQUS was used to analyze the mechanical behaviour of stud connectors. There are four main parts in push-out specimen: concrete blocks, steel plates, reinforced bars and studs. In order to save the calculation cost, only 1/4 model was built, as shown in Figure 1 (b). Symmetrical constrains were applied to simulate the real structure. Material nonlinearity was considered in the model. Dynamic explicit analysis method was used to analysis the push-out model. It’s more inexpensive than the implicit analysis, and also is very efficient to solve discontinuous and contact problems.
The concrete block, steel plate and stud were meshed with solid elements C3D8R, which is an 8-node brick element with reduced integration stiffness; each model has three translational degrees of freedom (DOF). The rebar was meshed with truss element T3D2, which has three degrees of freedom. The whole model used coarse mesh, with local fine mesh on stud and concrete block around stud connector to get accurate calculated results. The overall mesh size was 12mm, and the element size on stud and near stud was 3mm. The diameters of the rebar are 16mm and 20mm, which were assigned on the elements with different truss sections. Figure 2 shows the mesh models of different parts for push-out specimens.

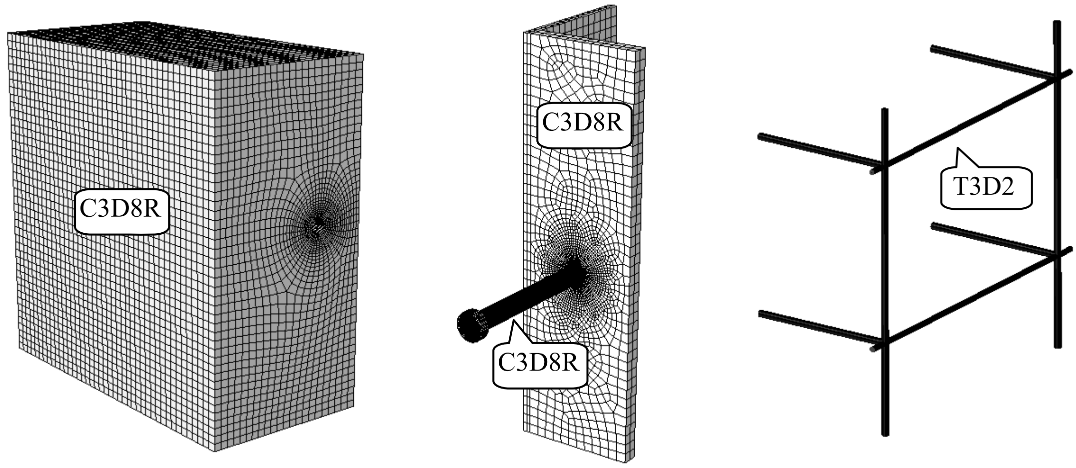

(a) Concrete (b) Steel and stud (c) Rebar

Figure 2. Finite Element Model

3.2 Material Models

3.2.1 Concrete material model

In this paper, concrete damaged plasticity model was used in the finite element model. It assumes the main two failure mechanisms are tensile cracking and compressive crushing of concrete material. The relationships between compressive stress (σ_c) and inelastic strain (ε_{in}) and between inelastic strain (ε_{in}) and damage (d_c) are needed to define for the compressive behaviour; the relationships between tensile stress (σ_t) and crack strain (ε_{ck}) and between crack strain (ε_{ck}) and damage (d_t) are needed to define for the tensile behaviour. The uniaxial stress-strain curves can be converted into stress versus plastic-strain curves by ABAQUS automatically [10].

(a) Concrete under compression
The nonlinear behaviour of concrete material under uniaxial compression is presented by an equivalent uniaxial stress-stress curve of concrete as shown in Figure 3.

The curve for concrete material under compression is modeled in three phases: the elastic phase, plastic ascending (hardening) phase and plastic descending (softening) phase [11,12].
The first part is initially assumed to be the elastic range till the stress value $0.4(f_{cm})$, where f_{cm} is the mean value of concrete cylinder compressive strength [13].
Elastic phase where $0<\varepsilon_c< 0.4 f_{cm}/E_c$: $$\sigma_{c1} = E_c\varepsilon_c \quad (1)$$
Hardening phase where $0.4 f_{cm}/E_c<\varepsilon_c <\varepsilon_{c1}$: $$\sigma_{c2} = \left(\frac{E_{ci}\frac{\varepsilon_c}{f_{cm}}-\left(\frac{\varepsilon_c}{\varepsilon_{c1}}\right)^2}{1+\left(E_{ci}\frac{\varepsilon_{c1}}{f_{cm}}-2\right)\frac{\varepsilon_c}{\varepsilon_{c1}}}\right)f_{cm} \quad (2)$$
Softening phase where $\varepsilon_c >\varepsilon_{c1}$: $$\sigma_{c3} = \left(\frac{2+\gamma_c f_{cm}\varepsilon_{c1}}{2f_{cm}} - \gamma_c\varepsilon_c + \frac{\gamma_c\varepsilon_c^2}{2\varepsilon_{c1}}\right)^{-1} \quad (3)$$

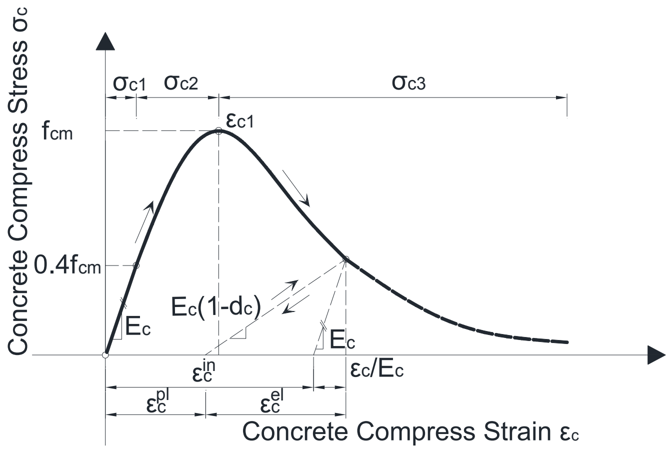

Figure 3. Concrete stress-strain relationship for uniaxial compression

The evolution of the compressive damage component d_c be calculated as follow equations, as Eq.(4), where b_c is a constant factor, $0 < b_c \leq 1$.

$$d_c = 1 - \frac{\sigma_c E_c^{-1}}{\varepsilon_c^{pl}\left(\frac{1}{b_c}-1\right)+\sigma_c E_c^{-1}} \tag{4}$$

The modulus E_{ci} in softening phase was defined as

$$E_{ci} = \frac{1}{2E_c}\left(\frac{f_{cm}}{\varepsilon_c}\right)^2 - \frac{f_{cm}}{\varepsilon_c} + \frac{3}{2}E_c \tag{5}$$

ε_{c1}——the strain at maximum compressive stress;
γ_c——the descent function

$$\gamma_c = l_{eq}/G_{cl} \tag{6}$$

Gcl: material crushing energy [12];
l_{eq}: the characteristic length of the respective FE integration point; which depends on type, quadrature rule and form of the element [14].
b_c: constant factor, which equals 0.7 [11];
E_c: Tangent modulus of elasticity of normal weight concrete;
ε_c: Compressive strain in the concrete;
σ_c: Compressive stress in the concrete;
f_{cm}: mean value of concrete cylinder strength of concrete at 28 days;
ε_c^{pl}: Compressive Plastic strain in the concrete;
To define the plasticity of concrete material under compression, there are several parameters needs to be defined in ABAQUS, as given in Table 2 [10].

ψ	E	σ_{b0}/σ_{c0},	Kc
30^o	0.1	1.16	0.667

Table 2. Parameters defined for plasticity of concrete

In the above table:
ψ: Dilation angle;
ε: Flow potential eccentricity;
σ_{b0}/σ_{c0}: the ratio of initial equibiaxial compressive yield stress to initial uniaxial compressive yield stress;
K_c: the ratio of the second stress invariant on the tensile meridian.

(b) Concrete material under tension
The nonlinear behaviour of concrete material under uniaxial tension is presented by an equivalent uniaxial stress-stress and stress-crack curves of concrete as shown in Figure 4. All stresses and deformations in the fracture process zone can be related to a fictitious crack opening *w* [15].

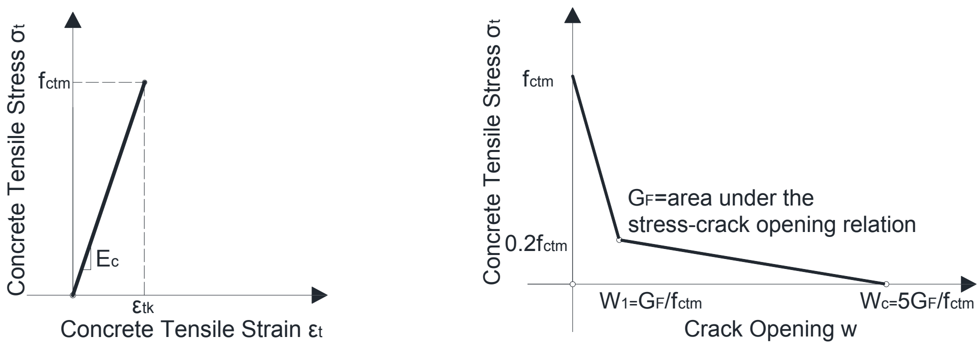

Figure 4. Concrete stress-strain and stress-crack opening relation for uniaxial tension

The tensile part curve can be assumed to increase linearly with respect to the strain until the concrete crack. There are two phrases in the curve of concrete under tension: the elastic phase and softening phase [12].
Tension Stiffening Set TYPE=GFI to define the post cracking behaviour by entering the failure stress, f_{ctm} and the fracture energy G_f [16].

$$G_f = 73 f_{cm}^{0.18} \tag{7}$$

Tension Damage Set TYPE=DISPLACEMENT to specify the tensile damage variable as a function of cracking displacement *w*.

3.2.2 Stud, structural and reinforcement steel materials

Two main mechanisms can cause the fracture of a ductile metal: ductile fracture due to the nucleation, growth, and coalescence of voids; and shear fracture due to shear band localization [10]. So ductile and shear criteria were used in stud material model to simulate the damage initiation. Fracture strain, stress ratio and strain rate were defined.
Two types of damage evolution, energy and displacement types, in conjunction with two softening laws, linear and exponential, were used to describe the progressive damage of stud material appropriately. Once the damage criterion is reached, the stiffness of the material degrades following the softening law. The elastic-plastic model of stud material is shown in Figure 5.

In this paper, all these parameters of stud's ductile behaviour were calibrated for the best agreement between analysis and experiment load-slip curves.

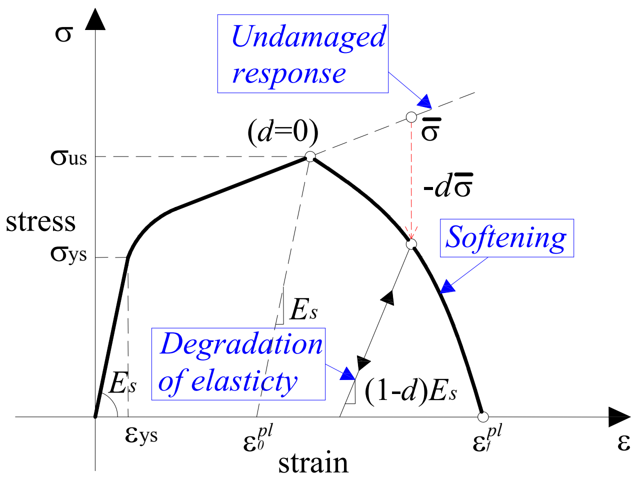

Figure 5. Elastic-plastic model of stud material with progressive damage

Tri-linear curve was used to simulate structural steel and reinforcement steel materials, as shown in Figure 6, and the material properties are shown in Table 3.

Materials	Steel Plate	Stud Connector	Rebar
Young's Elasticity Modulus E_s (MPa)	2.0E5	1.9E5	1.9E5
Poisson Ratio γ	0.3	0.3	0.3
The Failure Strength σ_y (σ_{ys}) (MPa)	340	370.4	370.4
The Ultimate Strength σ_u (σ_{us}) (MPa)	580	465.5	465.5

Table 3. Stud, structural and reinforcement steel material

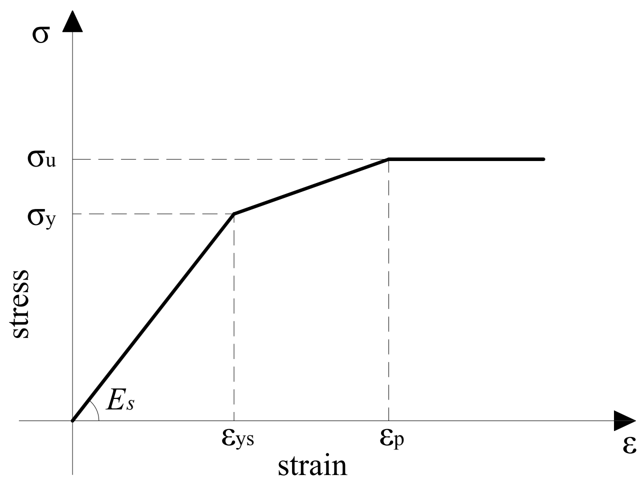

Figure 6. Structural Steel and Reinforcement Steel Material Models

3.3 Model Interactions and Constraints

The surface-to-surface formulation was used between steel beam surface, stud surfaces and concrete slab surface. The interaction between steel beam surface and concrete surface is frictionless, and ones between stud surfaces and concrete was set with friction coefficient 0.3, hard contact was defined in normal direction. Rebar elements were embedded in the concrete element, as shown in Figure 7.

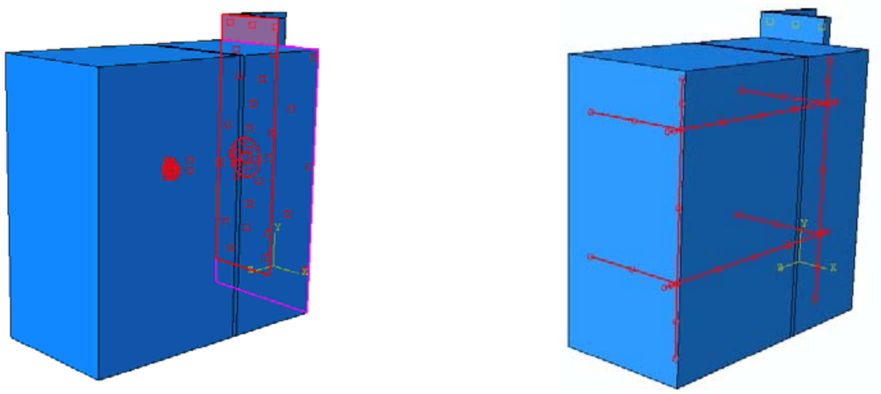

Figure 7. Simulation between steel, stud, rebar and concrete

3.4 Loading and Boundary Conditions

This model used displacement control to apply the push force; the compulsive displacement was applied on the top surface of steel plates. For the pull out force, load was put on the surface of steel beam against stud. The loading time was got by frequency analysis, and verified by experimental results.
The bottom surface of concrete block was fixed in all directions. And as 1/4 model, there are two different symmetrical constrain surfaces, as shown in Figure 8.

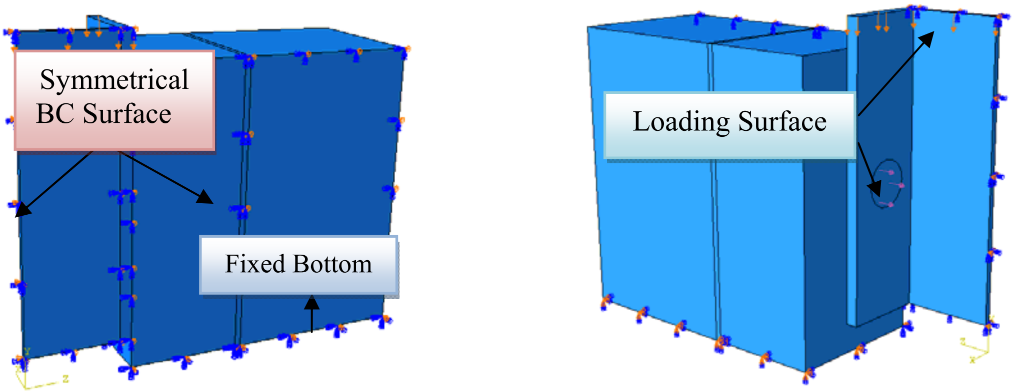

Figure 8. Boundary and Loading conditions

3.5 Analysis Results

Stud Deformation and stress and strain distribution of stud and concrete are shown in Figure 9. Under the push load been applied on the top of steel plates, the stud connectors have obviously shear deformation, and concrete under stud root has plastic strain; at the end, the elements of stud roots fail and the structure cannot take any more loads. Figure 9 (c) also shows the shank failure happened in push-out experiments.

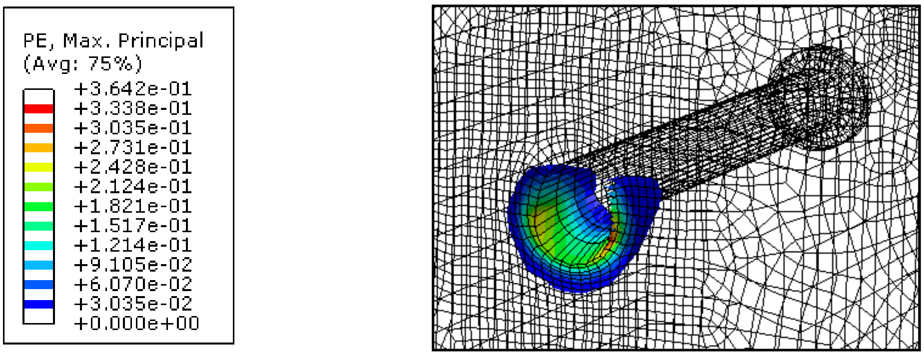

(a) Maximum Principle Plastic strain of concrete

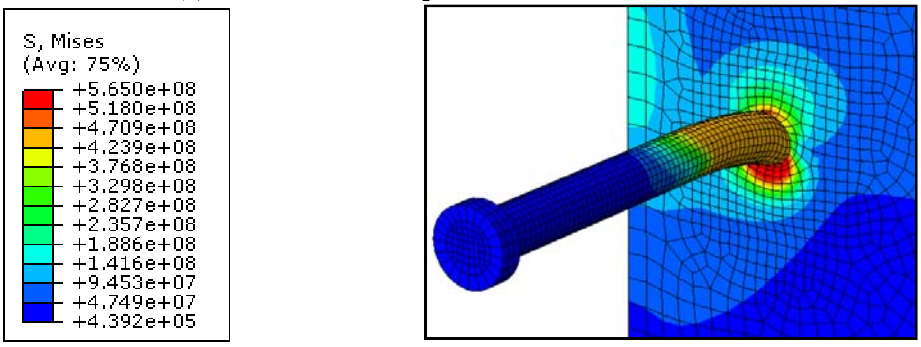

(b) Mises stress of stud

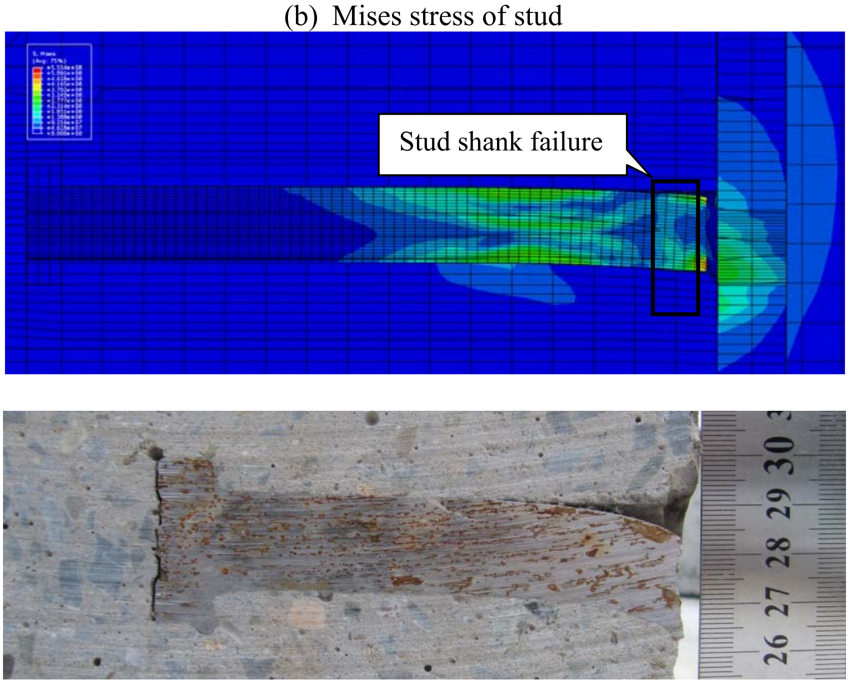

(c) Failure elements on stud

Figure 9. Stress and strain distribution for studs

4 Verification FE models with the experimental results

Figure 10 shows the comparison of experimental results and calculated results from the finite element models after parameters verification. It can be seen that the calculated load-slip curves have a good agreement with the experimental results. The finite element model can good estimate the experimental results of push-out specimens. Table 4 gives the damage parameters of stud material after verification.

Ductile damage			Shear damage		
Fracture strain	Fracture energy	Softening law	Fracture strain	Displacement at fail	Softening law
0.3	3000	Linear	0.8	1mm	Exponential

Table 4. Damage parameters of stud material

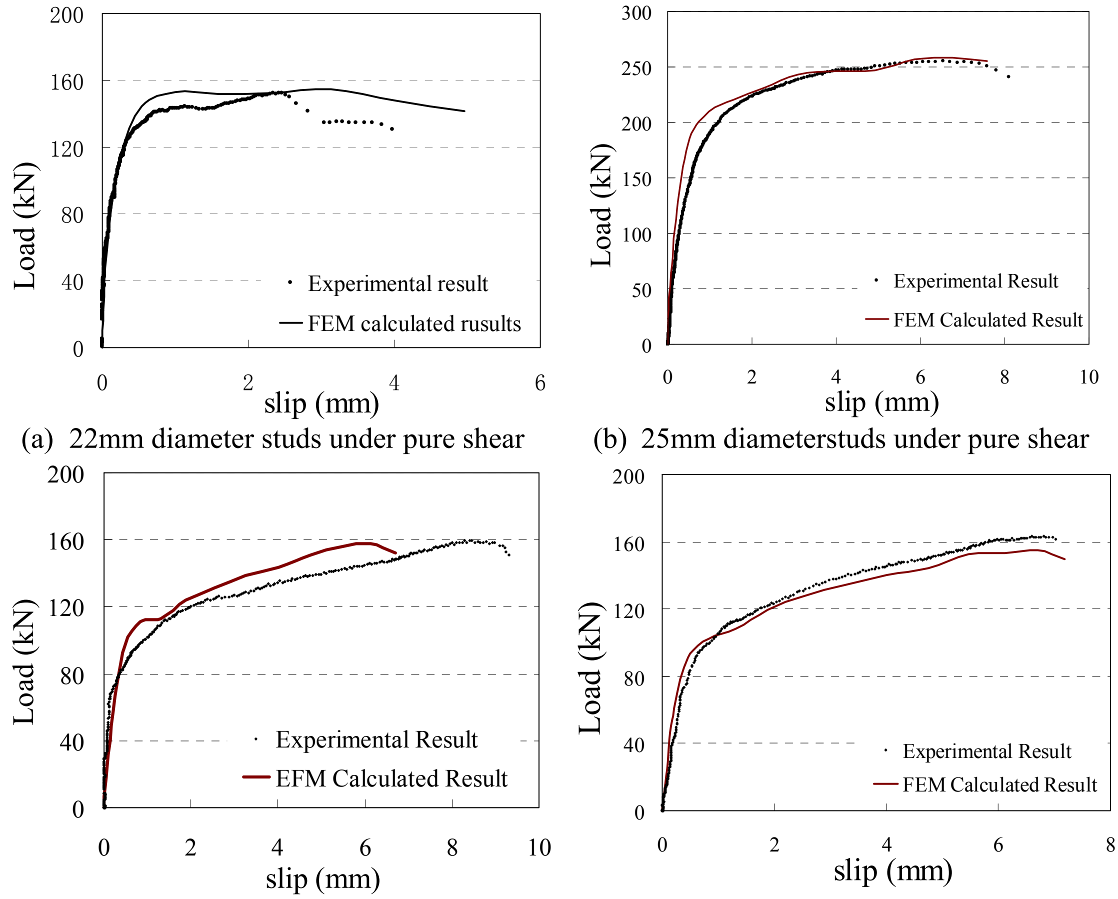

(a) 22mm diameter studs under pure shear

(b) 25mm diameterstuds under pure shear

(c) 22mm diameter studs under combined force (N_s=33.2kN)

(d) 22mm diameter studs under combined force (N_s=66.3kN)

Figure 10. Comparison of FEM calculated results with experimental results

5 Parametric study

5.2 General

According to different parameters as stud diameter, concrete strength and applied tensile forces, 11 nonlinear finite-element models was calculated as shown in Tab.5. According to the formula given by Hiragi.H (2003) [17], the calculated tensile resistance of 22mm studs with ultimate tensile strength 519MPa is 197.3kN. Different tension besides ones been used in the experimental specimens were chosen applied on the finite-element models.

Specimen	Stud Diameter d (mm)	Concrete Strength f_{ck} (MPa)	Tensile force N_s (kN)	Shear Resistance V_{su} (kN)
SS22-C60-N0	22	60	0	153.7
SS25-C40-N0	25	40	0	215.1
SS25-C50-N0	25	50	0	224.9
SS25-C60-N0	25	60	0	238.5
SS25-C70-N0	25	70	0	250.6
SS25-C80-N0	25	80	0	259.3
SS30-C60-N0	30	60	0	315.3
SS22-C50-N33.2	22	50	33.2	157.4
SS22-C50-N45	22	50	45	155.7
SS22-C50-N66.3	22	50	66.4	155.2
SS22-C50-N90	22	50	90	153.7

Table 5. Parametric study of finite element models

5.3 Stud diameter and concrete strength

From former research we can know that stud diameter and concrete strength are the main influence factors to the shear resistance of stud connectors. In this paper, different concrete strengths were applied in the finite element models with 25mm studs as 40MPa, 50MPa, 60MPa, 70MPa and 80MPa, and different stud diameters were considered as 22mm, 25mm and 30mm. The calculated load-slip curves are shown in Fig. 11. As stud diameter and concrete strength increases, the shear resistance increases. The stud diameter has bigger effect than concrete strength to the shear resistance of stud connectors. As the diameter of stud connector changes from 22mm to 25mm, the shear resistance increases 55.14%; from 25mm to 30mm, the shear resistance increases 32.2%. In the FE models, the concrete strength was considered from C40 to C80, the shear resistance of stud connectors increases about 5% as from C40 to C50, C50 to C60, and so on. The diameter of stud has bigger influence to the shear resistance of stud connectors than the concrete strength.

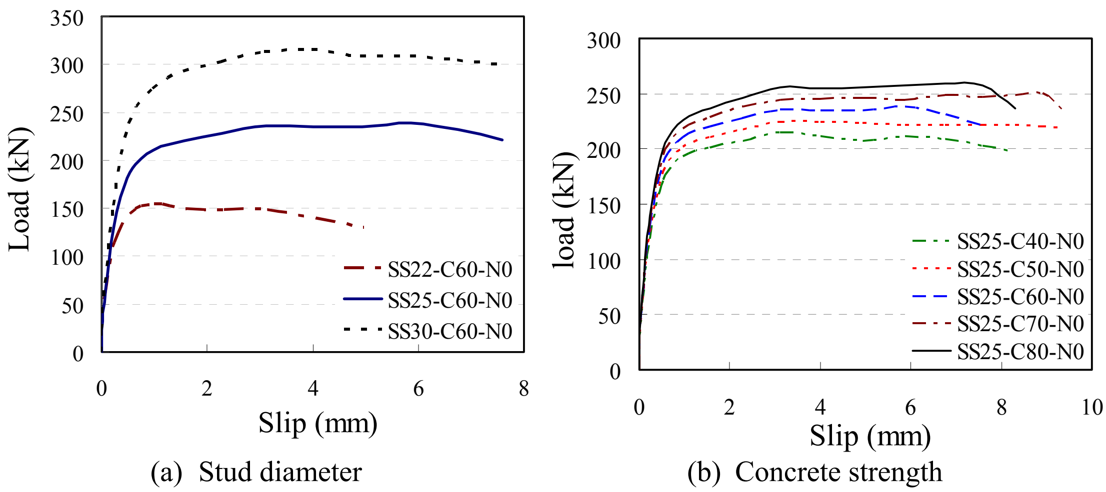

Figure 11. Parametric Analysis

5.4 Different tensile strength

Figure 12 shows the load-slip curves of FE models under combined forces. The tensile forces were considered as 33.2 kN, 45 kN, 66.3 kN and 90 kN separately. And the shear resistances under tension are listed in Table 5. From the curves we can know that when the load-slip curves first enter plastic phrase, the loads taken by the specimens decreases as tensile force increases; the ultimate shear resistance of specimens under combined tensile and shear forces has the same trend, not as obviously as the initial phrase.

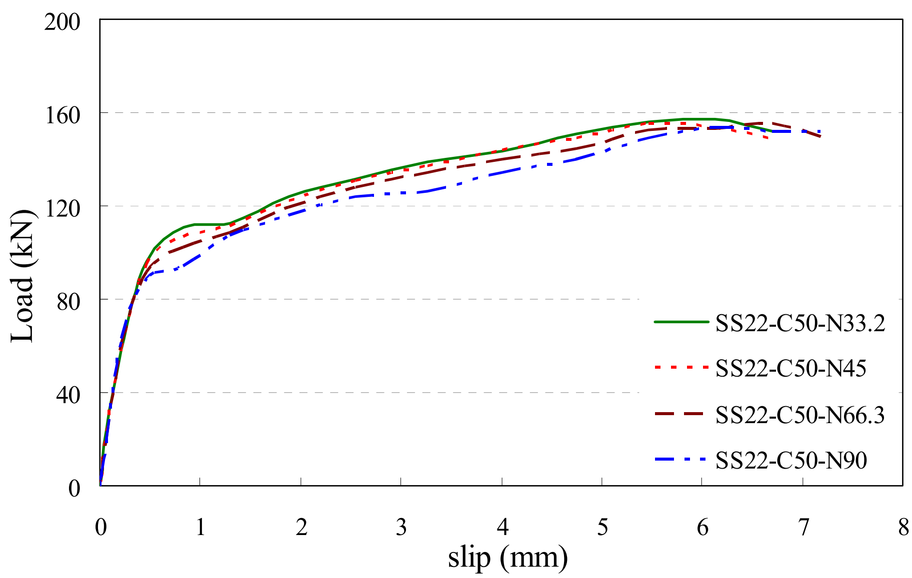

Figure.12 Effect of tensile strength

6 Conclusions

Nonlinear finite-element models were built in this paper to study on the mechanical behaviour of stud connectors.

(1) Concrete damage-plastic model was used in the FE models; in which three different phases were considered for the concrete equivalent uniaxial stress-strain curve under compression as: elastic phase, plastic ascending (hardening) phase and plastic descending (softening) phase.

(2) For stud material, ductile and shear criteria were applied in stud material model to simulate the damage initiation of studs, and energy type damage evolution with exponential softening laws to describe the progressive damage.

(3) The calculated load-slip curves were compared with the experimental load-slip curve, which proves that the nonlinear finite-element model after verification can good estimate the load-slip curve of stud connecter under pure shear and combined forces.

(4) An extensive parametric study of 11 specimens was performed by considering different stud diameters, concrete strengths and applied tensile forces. The shear resistance of stud connectors increases as stud diameter and concrete strength increase, and the stud diameter has bigger influence to the shear resistance than the concrete strength. Under combined forces, the shear resistance of stud connector decreases as the applied tensile force increases.

Acknowledgements

The authors would like to thank Mr. Yao Zeng from Tongji University for his technical support in the finite element analysis with ABAQUS.

References

[1] BS EN 1994-2. "Eurocode-4: Design of composite steel and concrete structures, Part 2: General rules and rules for bridges". 2005.

[2] Driscoll G. C, and Stutter, R. G. "Research on Composite Design at Lehigh University". In "Proceedings of Conference", AISC, May, 1961.

[3] Stutter, R. G, and Driscoll, C. C. "Flexural Strength of Steel-Concrete Composite Beams", in "Journal of the Structural Division", ASCE, Vol. 91, No. ST2, April 1965.

[4] AASHTO LRFD. "Bridge design specifications. 3rd ed". American Association of State Highway and transportation Officials; 2004.

[5] GB50017-2003. "Code for design of steel structures". Ministry of Construction of China, Beijing: China Planing Press, 2003

[6] Ellobody E. "Finite element modeling of shear connection for steel-concrete composite girders". Ph.D. thesis. Leeds: School of Civil Engineering, The University of Leeds; 2002.

[7] Lam D, Ellobody E. "Behavior of headed stud shear connectors in composite beam". In "Journal of Structural Engineering", ASCE 2005; 131(1): 96-107.
[8] Ellobody E, Young B. "Performance of shear connection in composite beams with profiled steel sheeting". In "Journal of Constructional Steel Research" 2006; 62: 682-94.
[9] Huu Thanh Nguyen, Seung Eock Kim. "Finite element modeling of push-out tests for large stud shear connectors". In "Journal of Constructional Steel Research", 65 (2009), 1909-1920.
[10] "ABAQUS analysis user's manual", Volume III: Materials. USA, 2010.
[11] V. Birtel, P. Mark. "Parameterised finite element modeling of RC beam shear failure, analysis user's manual", Volume III: Materials. USA, 2010.
[12] Krätzig, W. B., "Pölling, R.. An elasto-plastic damage model for reinforced concrete with minimum number of material parameters". In "Computers & Structures". 82, 2004: 1201-1215.
[13] BS EN 1992-1-1. "Eurocode-2: Design of concrete structures, Part 1-1: General rules and rules for buildings". 2004.
[14] Oliver J. "A consistent characteristic length for smeared cracking models". In "International Journal for Numerical Methods in Engineering". 1989; 28: 461-74.
[15] Fédération Internationale du Beton (fib), "Constitutive modelling of high strength/high performance concrete - STAR", Bulletin 42, January 2008
[16] Fédération Internationale du Beton (fib). "fib Bulletin 55: Model Code 2010", First complete draft –Volume, 2010
[17] Hirokazu Hiragi, Shigeyuki Matsui, Takashi Sato, et al. "Pull-out and shear strength equations for headed studs considering edge distance". In "Structural Engineering/Earthquake. Engineering"; Vol.20, no.1, 2003: pp.69-80.